



Check for updates

AUTHORS:

Arwa El-Naeem¹
Sahar Abdalla¹
Ibrahim Ahmed¹
Gihan Alhassan²

AFFILIATIONS:

¹Department of Chemistry, University of Khartoum, Khartoum, Sudan
²Department of Botany, University of Khartoum, Khartoum, Sudan

CORRESPONDENCE TO:

Sahar Abdalla

EMAIL:

sahar.abdalla@uofk.edu

DATES:

Received: 07 Mar. 2021

Revised: 15 June 2021

Accepted: 21 June 2021

Published: 27 Jan. 2022

HOW TO CITE:

El-Naeem A, Abdalla S, Ahmed I, Alhassan G. Phytochemicals and in silico investigations of Sudanese roselle. *S Afr J Sci.* 2022;118(1/2), Art. #10383. <https://doi.org/10.17159/sajs.2022/10383>

ARTICLE INCLUDES:

Peer review
 Supplementary material

DATA AVAILABILITY:

Open data set
 All data included
 On request from author(s)
 Not available
 Not applicable

EDITORS:

Teresa Coutinho
Salmima Mokgehele

KEYWORDS:

roselle, polyphenols, anthocyanins, gout, xanthine oxidase

FUNDING:

None

Phytochemicals and in silico investigations of Sudanese roselle

We analysed four different Sudanese roselle samples for their potential as novel xanthine oxidase (XO) inhibitors. Phytochemical screening showed the presence of polyphenols, flavonoids, organic acids, saponins and sterols in all samples. Liquid chromatography with tandem mass spectrometry (LC-MS/MS) was used to identify and characterise five anthocyanins in all samples: cyanidin-3-glucoside (cy-3-glu), delphinidin-3-sambubioside (dp-3-sam), cyanidin-3-rhamnoside (cy-3-rhm), delphinidin-3-rhamnoside (dp-3-rhm) and pelargonidin-3-glucoside (pg-3-glu). Identification of cy-3-rhm, dp-3-rhm and pg-3-glu confirmed the selectivity and sensitivity of LC-MS as a powerful technique for identifying anthocyanins. In silico studies of the identified anthocyanins were performed to explore their promising inhibitory activity toward XO. Interactions between the ligand and the enzyme were via the H-bond, and hydrophobic (π -alkyl, π -sigma and alkyl) and/or electrostatic (π -cation) bonds. Inhibition of the anthocyanins was compared with that of topiroxostat, a commercial drug for hyperuricaemia. Dp-3-rhm was the most active inhibitor with a binding energy of ca. -10.90 kcal/mol compared to topiroxostat's binding energy of ca. -8.60 kcal/mol. The good inhibition results obtained from anthocyanins toward XO suggest their application as a drug candidate to treat gout and other diseases related to the activity of XO.

Significance:

- Sudanese roselle is rich in phytochemicals, particularly polyphenols and anthocyanins. The isolated anthocyanins in this study were explored as novel potential XO inhibitors. Further pharmacological and clinical studies are necessary for the development of new potential anthocyanin drugs to treat gout and other diseases related to XO increased activity such as hypertension.

Introduction

Hibiscus sabdariffa L. – commonly known as roselle, hibiscus and karkade – is an annual or perennial plant that grows in tropical and subtropical regions of the world including Sudan.¹⁻³ Its calyces are characterised by a sour taste, brilliant red colour, and pleasant aroma that gives the plant its commercial importance.^{3,4}

Roselle, like other plants, possesses phytochemical compounds such as tannins, saponins, glycosides, phytosterols, minerals, organic acids, and antioxidants like polyphenols, flavonoids, and vitamins.^{2,4,5} These compounds occur naturally in different parts of the plants and they are characterised by their protective and preventive properties against several diseases.⁶

The calyces of roselle are rich in anthocyanin pigments; anthocyanins are water-soluble plant pigments responsible for providing the colours to almost all plant tissues.⁷⁻⁹ In various plant tissues, anthocyanins vary in amount and type according to composition and chemical structures.⁷ Plants containing anthocyanin extracts may have up to 10 different anthocyanins in addition to other flavonoids.¹⁰ All anthocyanins share a basic common structure of glycosylated anthocyanidin as illustrated in Figure 1. The aglycone part (anthocyanidin) is a polyhydroxy or a polymethoxy derivative of 2-phenyl-benzopyrylium or flavylium salt.^{7,8} All identified anthocyanins are based on six major anthocyanidins: cyanidin, delphinidin, pelargonidin, peonidin, petunidin, and malvidin.⁷⁻⁹

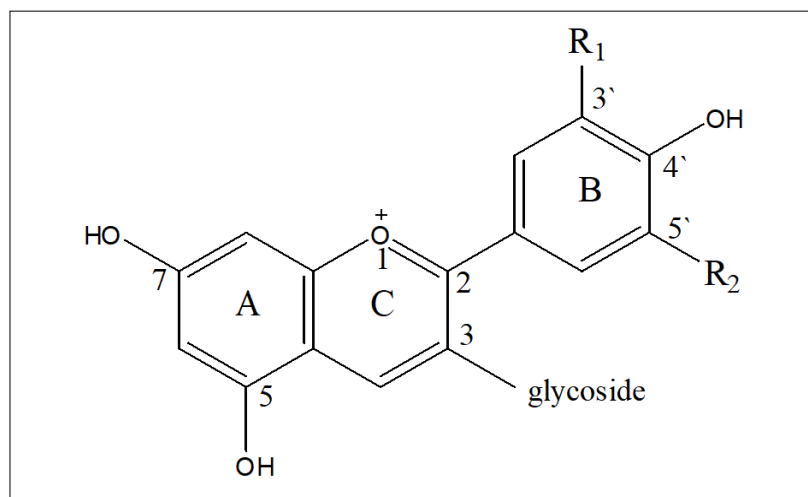


Figure 1: General structure of anthocyanins.

© 2022. The Author(s). Published under a Creative Commons Attribution Licence.

Identification of anthocyanins is usually carried out using chromatographic, spectrophotometric and capillary electrophoresis analytical methods.^{3,9} The most commonly used technique is hyphenated liquid chromatography–mass spectrometry (LC-MS), as it is the most efficient due to its high selectivity and sensitivity.⁹

The red colour of roselle calyces is attributed to the presence of: dp-3-sam, cy-3-sam, dp-3-glu and cy-3-glu anthocyanins.⁵ Dp-3-sam and cy-3-sam anthocyanins are responsible for the reddish-violet colour of roselle.^{3,11}

Characterisation of anthocyanins is essential due to their numerous curative and preventive properties which make them potential pharmacological and therapeutic agents.^{8,12} Dp-3-sam and cy-3-sam are considered to be antihypertensive, antioxidant, and hypocholesterolaemic. There is a correlation between the antioxidant activity and the intensity of the red colour of the calyces.¹³ Anthocyanins play an indirect role as antioxidants by inhibiting some enzymes such as lipoxygenases, nicotine amide adenine dinucleotide phosphate (NADPH) oxidase and xanthine oxidase (XO).^{7,14}

In the present work, we put special emphasis on the inhibition of XO by anthocyanins. XO belongs to the molybdenum protein family of enzymes. Structurally, XO is composed of two identical monomers. Each monomer contains one molybdenum atom, one of the flavin adenine dinucleotides, and two iron-sulfur (2Fe-S) centres of the ferredoxin type including two separated substrate-binding sites, i.e. the purine binding site and the flavin adenine dinucleotides cofactor site; both binding sites are vulnerable to inhibitors.¹⁵ To our knowledge, XO is a highly versatile enzyme, which is widely distributed among different animal kingdom species.¹⁶ Furthermore, XO catalyses the metabolic conversion of purine bases to uric acid^{15,16} to produce superoxide radicals as well as

hydrogen peroxide reactive oxygen species¹⁵. Thus, an increase in the activity of the enzyme leads to accumulation of uric acid and reactive oxygen species^{15,17}, and results in several diseases. For example, hyperuricaemia and gout are the main chronic diseases associated with increased activity of XO, as well as several diseases including, but not limited to: hypertension, metabolic syndrome, cardiovascular disease, diabetes, obesity, cancer and hyperlipidaemia.¹⁵⁻¹⁷

The well-known traditional uses of roselle for treating hypertension as well as some other diseases, encouraged us to examine the inhibitory effect of anthocyanins in roselle towards XO by aid of molecular docking in the current work. The structures of the compounds obtained from the LC-MS analysis that used docking ligands are illustrated in Figure 2.

To validate the inhibitory activity of the anthocyanin ligands towards XO, we compared their activity with that of topiroxostat, the standard drug for treatment of hyperuricaemia. The structure of topiroxostat is represented in Figure 3.

Experimental

Sample preparation

A total of four dried samples of roselle calyces, including both red and white calyces, were collected from different parts of Sudan. After selection, each sample was cleaned from agricultural residues and ground to a fine powder using an electrical grinder (Monolex, France); the powder was well homogenised, packed in polyethylene bags, and stored at room temperature (20–30 °C).

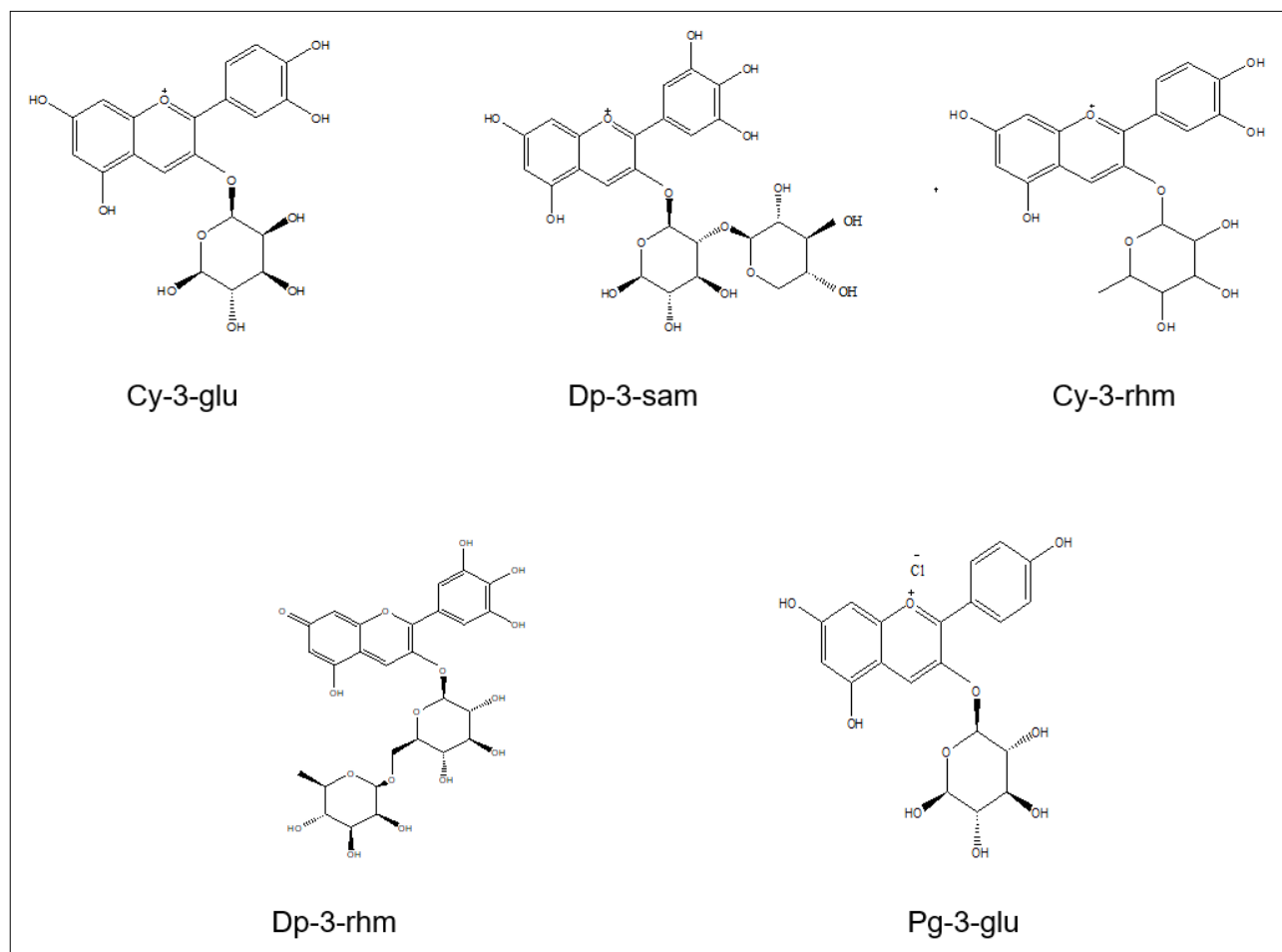


Figure 2: Chemical structures of the anthocyanin ligands.

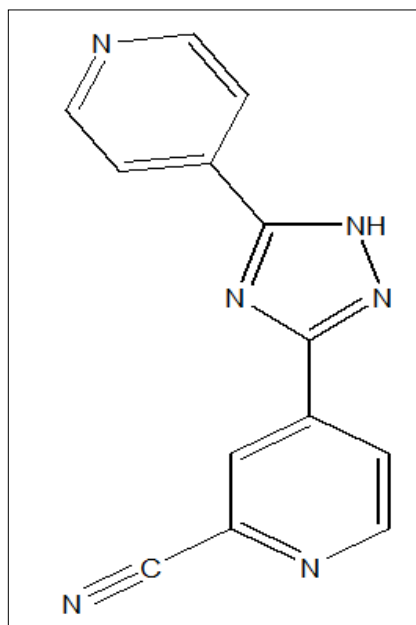


Figure 3: The chemical structure of topiroxostat (FYX-051).

Chemicals

All chemicals were of analytical grade except those used in LC-MS analysis which were HPLC-grade.

Phytochemical screening

Preparation of extracts

The extract was prepared according to Wrolstad et al.'s¹⁸ alternative protocol with some modifications in the purification step. The purification was established by simple liquid-liquid extraction using an organic non-polar solvent (petroleum ether) and (0.01% (v/v) HCl) acidified methanol to remove water-insoluble impurities. The desired layer was reserved, the solvent was evaporated using a rotatory evaporator (Heidolph Laborota 4000 efficient HB digital, Germany) and allowed to air dry for 3–4 h. The attained gummy extract was used for all the phytochemical qualitative and quantitative analyses after dissolving in 1–2 cm³ methanol for each qualitative test.

Preliminary screening

Qualitative analysis was carried out according to methods described by Harborne¹⁰ and Sofowara¹⁹ via simple test tube tests. These are the test for polyphenols (FeCl₃ test), test for flavonoids (AlCl₃ test), test for sterols (H₂SO₄ test), test for saponins (Frothing test), and test for anthraquinones (KOH test).

Thin-layer chromatography

An amount of 10 mg from the gummy powdered extract of each of the samples was dissolved in 1 cm³ of methanol and, using a capillary tube, spots were made from each sample extract on an aluminium sheet of pre-coated silica gel thin-layer chromatography plates, then elution was carried out in a covered thin-layer chromatography chamber using the mobile phase of a mixture of chloroform and methanol (7:3 v/v) according to Harborne¹⁰. The procedure was repeated on two other plates.

After performing the elution, plates were examined immediately in daylight, then sprayed with chemical reagents and visualised under a UV lamp (at 365 nm). Bromocresol green was the spray reagent employed for detection of organic acids, while AlCl₃ was used for detection of flavonoids.²⁰

Quantitative analysis

Total phenolic content was measured using Folin–Ciocalteu's reagent as described by Wolfe et al.²¹ Total flavonoid and total anthocyanin contents were measured according to Shanmukha et al.²² and Pacôme et al.⁶, respectively.

For total phenolic and flavonoid contents, absorbance was measured at 765 nm and 510 nm, respectively, against a reagent blank using a Jenway 7205 UV/Vis double-beam spectrophotometer. The concentrations of phenolics and flavonoids in the test sample were determined and expressed as gram equivalent of gallic acid (g GAE) and quercetin per gram of air-dried extract (g ADE), using a standard calibration plot for each individually. All measures were performed in duplicate.

Determination of total anthocyanins

Total anthocyanin content was measured at an absorbance of 530 nm using a Jenway 7205 UV/Vis spectrophotometer against the blank; total anthocyanin content was estimated as cyanidin-3-glucoside at 530 nm using a molar extinction coefficient of 26 900 L/mol/cm and molar mass (449 g/mol) and was expressed as cyanidin-3-glucoside (g cy-3-glu)/(100 g of air-dried extract).⁶

LC-MS/MS identification

Anthocyanin extraction was carried out using 250 cm³ acidified methanol by Soxhlet apparatus² at a temperature of 50–55 °C. The extract was purified by simple liquid/liquid extraction after reducing the extract volume using the rotatory evaporator (Heidolph Laborota 4000 efficient HB digital, Germany).

Anthocyanins were identified in the purified sample extracts using LC-MS/MS with a UPLC-Q-TOF-MS (XEVO-G2 QTOF YCA119, Waters, using Acquity UPLC HS T3 (100 × 2.1 mm, 1.8 μm; Waters) column maintained at 45 °C in a column oven in the LC-MS Laboratory, Beijing University of Chemical Technology BUCT, China. The analysis was carried out according to the method described by Cahliková et al.²³ with some modifications. The conditions of the chromatographic run were as follows: 0–1 min: 90% A and 10% B, 1–5 min: 85% A and 15% B, 5–10 min: 40% A and 60% B, 10–13 min: 0% A and 100%B, 13–15 min: 90% A and 10% B. Gradient mobile phase composed of water acidified with 0.1% formic acid (solvent A) and acetonitrile (solvent B). The flow rate and sample injection volume were 0.4 cm³/min and 3.00 μL, respectively.

The ion source of the quadrupole time-of-flight (Q-TOF) detector was set at the positive electrospray ionisation polarity mode. The optimum conditions of the Q-TOF system, performed in the resolution mode, were: capillary voltage: +3.000 kV, ion source temperature: 100 °C, extractor: 4.0 V; RF lens: 0.3 V, mass range m/z: 50 to 2000 Da, nitrogen as the desolvation gas at a flow rate of 800 L/h and at a temperature of 400 °C. Nitrogen was used also as the cone gas (20 L/h), and argon as the collision gas. The cone voltage, collision energy, and well time were carefully optimised for each compound and transition individually (cone voltage set at 4/30 V, collision energy set finally at 6 eV). The software used for the MS control and data gathering was Mass Lynx 4.1.

Molecular docking

Molecular docking is a method used to screen for the ability of specific small compounds (ligands) to fit into a previously identified therapeutic target (the receptor; usually a protein enzyme).^{24,25} Several docking programs can be used: AutoDock Vina, GOLD, and MOE-Dock are top ranked with the best scores.²⁵ We used the AutoDock Vina program²⁶ for the docking of anthocyanin ligands to the active site of the XO enzyme, after performing the required preparations.

First, the protein crystal structure and ligand 3D structures were downloaded from RCSB Protein Data Bank²⁷ (1FIQ PDB code) and PubChem online databases²⁸, respectively. Then the suitable binding site of the protein was obtained using Chimera software²⁹ and the ligands were converted via Open Babel software³⁰ from SDF format to pdbqt. Thereafter, using autodock tools³¹, all water molecules in the protein

pdb file were removed, hydrogen atoms were added, and the grid box dimensions were set, then the file saved as pdbqt. Ligands were prepared by detecting torsions for each structure and saved as a pdbqt file. The AutoDock Vina order was then created after preparing the configuration files. The process was repeated for each docking trial for all ligands.

Data analysis

The obtained (out.pdbqt) file for each ligand was visualised using discovery studio³² and pymol³³ visualisation programs.

Results and discussion

Phytochemical screening

Qualitative analysis

Our results show that roselle is rich in phytochemicals, especially anthocyanins, in agreement with the results of previous studies.³⁻⁵ The general screening of some phytochemical constituents detected the presence of polyphenols, flavonoids, saponins, and sterols, and an absence of anthraquinones. Although the different roselle types had similar phytochemical constituents, the red type exhibited higher contents of polyphenols and flavonoids than the white type. Table 1 reports the phytochemical screening tests for four samples of roselle.

The sour taste of roselle is due to the presence of organic acids.^{3,4} Flavonoids, particularly the anthocyanins, are the compounds that give roselle its importance and its colour.³⁻⁵ To investigate the presence of organic acids and flavonoids, thin layer chromatography was performed and the results are shown in Table 2.

The presence of different organic acids is confirmed by spots at different R_f values. In contrast, similar types of flavonoids are separated at equal R_f values for all samples. Therefore, it is worth mentioning that the solvent system used, i.e. chloroform: methanol 7:3, is suitable for separation of organic acids but not the best for separation of flavonoids. Our finding of the presence of phytochemical compounds in roselle is in good agreement with previous investigations.^{2,5,6,34}

Quantitative analysis

Result of the quantitative analysis of polyphenols, flavonoids, and anthocyanins in roselle are presented in Table 3. Anthocyanins have the lowest concentration among the three measured phytochemical groups, followed by flavonoids and then polyphenols. All samples show high polyphenolic and flavonoid contents and therefore express the antioxidant character of roselle, in agreement with Riaz et al.⁵

Sample 1 (light red colour) has the lowest phenolic and flavonoid contents of all the samples, while Sample 3 (brown-white colour) has the lowest anthocyanin content. Sample 4 has the highest phenolic content, but lower anthocyanin content and Sample 2 (dark red), which is characterised by its brilliant violet-red extract, has the highest flavonoid and anthocyanin contents.

Table 1: Phytochemical screening tests

Constituents	Reagents	Observation	Samples			
			1	2	3	4
Polyphenols	FeCl ₃	Samples 1 and 2: dark green Samples 3 and 4: light green	++ve	++ve	+ve	+ve
Flavonoids	AlCl ₃	Samples 1 and 2: blue Samples 3 and 4: yellow	++ve	++ve	+ve	+ve
Anthraquinones	KOH	Yellow	-ve	-ve	-ve	-ve
Sterols	CHCl ₃ and H ₂ SO ₄	Reddish violet	+ve	+ve	+ve	+ve
Saponins	Boiled H ₂ O	Formation of frothing persisted on warming	+ve	+ve	+ve	+ve

Table 2: Thin layer chromatography results

Constituents	Spray reagent	Observation
*Flavonoids	AlCl ₃	Bright yellow spots under 365 nm wavelength
*Organic acids	Bromocresol green	Yellow spots in blue background under daylight

*Chloroform: methanol 7:3 mixture solvent system

In contrast to the above-mentioned qualitative test of polyphenols and flavonoids, the red samples show lower values of polyphenols and flavonoids than the white samples in the quantitative test. The red colour affects the colour intensity in the qualitative tests, appearing higher than the actual amount, whereas the quantitative analysis gives the exact concentrations of polyphenols and flavonoids.

Our findings show that Sudanese roselle is rich in polyphenols and flavonoids and the total anthocyanin content is high³ compared to Egyptian⁴ and Abidjan⁶ roselle.

LC-MS/MS Identification of anthocyanins

LC-Q-TOF-MS identification of anthocyanins revealed the presence of five anthocyanin types in all samples. The formulae and molecular weights of the identified compounds match the theoretical molecular weight values of anthocyanins obtained from PubChem.²⁸ Table 4 presents the chemical formulae, and the measured and theoretical values of the molecular weights of the identified anthocyanins.

The presence of five anthocyanin types in our results confirms the validity of the LC-MS technique as the most powerful and suitable technique for analysing anthocyanins, due to its high sensitivity and selectivity. These findings are in accordance with studies considering Sudanese roselle using the same technique which identified dp-3-rhm^{23,35}, cy-3-rhm^{23,35}, and pg-3-glu anthocyanins³⁵. However, these anthocyanins were not identified in Abidjan roselle analysed using non-hyphenated HPLC.^{6,36} Analysis of Sudanese roselle using thin-layer chromatography expressed the presence of two anthocyanins: dp-3-sam and cy-3-sam.³

Molecular docking

The inhibition property of the five obtained anthocyanins was tested against XO. According to our docking results, all obtained anthocyanins manifested strong inhibitory activity toward XO, superior to the standard drug (topiroxostat). All ligands exhibited low binding energies, ranging from -10.9 to -9.6 kcal/mol. The binding energies are shown in Table 5.

The variation of the binding energy values can be directly related to the anthocyanin types, i.e. anthocyanins with different glucoside, or different position or type of substituent group. This finding supported the idea that different anthocyanins result in different molecular fittings into a binding

Table 3: Quantitative analysis of polyphenol, flavonoid, and anthocyanin contents (in g/g%) in methanolic extracts of roselle

Phytochemical group	Contents in (g/g%)						
	1	2	3	4	Ref [3]	Ref [4]	Ref [6]
Polyphenols	6.77±0.19	9.81±0.49	6.98±0.07	13.15±0.42	–	3.70	0.74
Flavonoids	2.12±0.03	8.70±0.06	6.24±0.03	8.23±0.34	–	–	0.35
*Anthocyanins	0.32±0.02	1.03±0.03	0.043±0.00	0.09±0.02	(0.97,1.0)** and 0.001***	0.622	1.65

Values are means of duplicate determinations ($n = 2$) ± standard deviation
 *Total anthocyanins measured as cyanidin-3-glucoside; **red samples, ***white samples

Table 4: Liquid chromatography quadrupole time-of-flight mass spectrometry (LC-Q-TOF-MS) identification

Measured m/z	Theoretical m/z	Chemical formula	Name of the identified compound
449.1084	449.388	$C_{21}H_{21}O_{11}^+$	Cy-3-glu
597.1456	597.502	$C_{26}H_{29}O_{16}^+$	Dp-3-sam
595.1663	595.530	$C_{21}H_{21}O_{10}^+$	Cy-3-rhm
611.1612	610.521	$C_{27}H_{30}O_{16}^+$	Dp-3-rhm
433.415	433.389	$C_{21}H_{21}O_{10}^+$	Pg-3-glu

Table 5: Binding energies of the anthocyanin–XO and topiroxostat–XO complexes

Docked ligand	Binding energy (kcal/mol)
Dp-3-rhm	-10.90
Dp-3-sam	-10.50
Cy-3-rhm	-10.30
Pg-3-glu	-9.60
Cy-3-glu	-9.50
Topiroxostat	-8.60

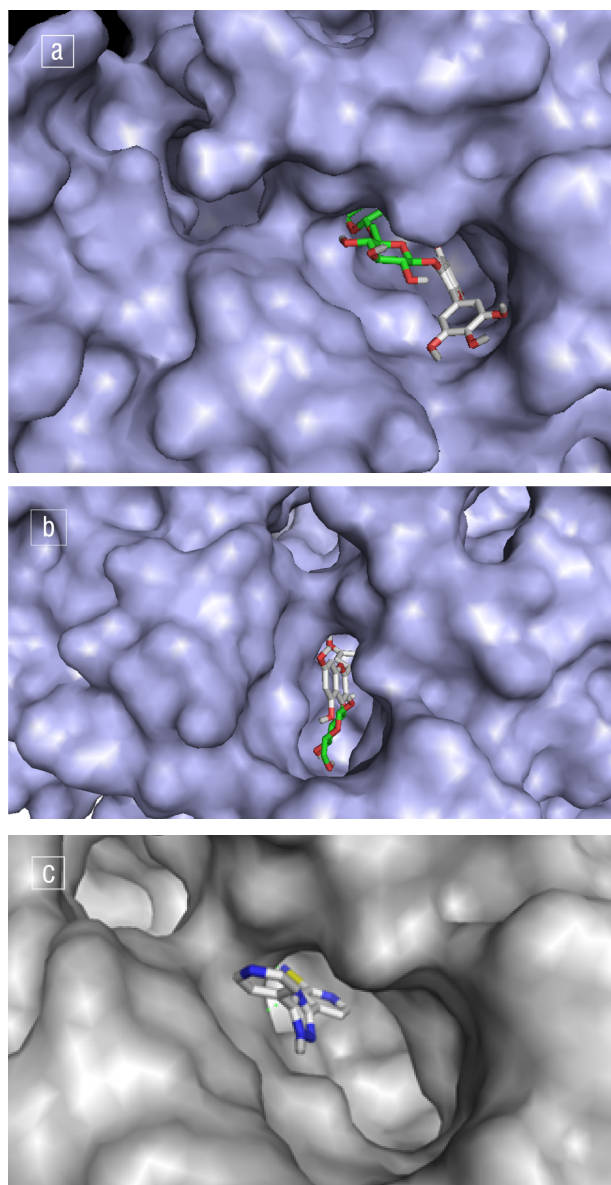
site.⁷ Fittings of dp-3-rhm, cy-3-glu and topiroxostat into the binding site are shown in Figure 4.

The small values of the binding energy may be due to the presence of free hydroxyl groups in the ligand structures that are available to involve in hydrogen bonds, as proposed by Wallace et al.¹⁴ The source of these hydroxyl groups is either one or more anthocyanidin rings (B and/or C) or glucoside moiety. For instance, Figure 4 illustrates the binding of the hydroxyl cy-3-glu.

In addition to the binding of the OH group via H-bonds, the π -system of the rings contributes to the interaction and enhances the inhibition of XO. The interaction is either hydrophobic (π -alkyl, π -sigma and alkyl) or electrostatic (π -cation). Figure 5 exhibits the different interactions in cy-3-glu.

The amino acid residues' binding sites THR354 and ARG394 are bonded to topiroxostat with a hydrogen bond of length 2.78 Å, and carbon hydrogen bond of length 3.55 Å. THR354 and ARG394 are bonded with dp-3-sam by hydrogen bonds of lengths 2.16 Å and 2.42 Å. THR354 interacts with cy-3-rhm and dp-3-rhm by 2.12 Å and 2.27 Å hydrogen bonds, respectively.

Different basic structures between topiroxostat and the anthocyanins allow different bindings. Topiroxostat, illustrated in Figure 2, lacks


Figure 4: Fittings of (a) dp-3-rhm, (b) cy-3-glu and (c) topiroxostat into the flavin adenine dinucleotide binding site in xanthine oxidase inhibition.

glucoside moiety and substituted hydroxyl groups which constitute the most important moieties in the binding interactions of anthocyanins.

Dp-3-rhm obtains the most stable conformer with a binding energy of ca -10.9 kcal/mol; whereas the complex with the highest binding energy of ca. -9.50 kcal/mol is cy-3-glu, which has a lower binding energy than topiroxostat (-8.6 kcal/mol).

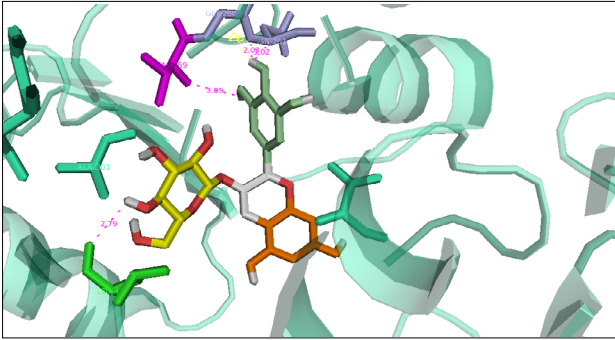


Figure 5: Cy-3-glu docking binding interactions through hydroxyl groups.

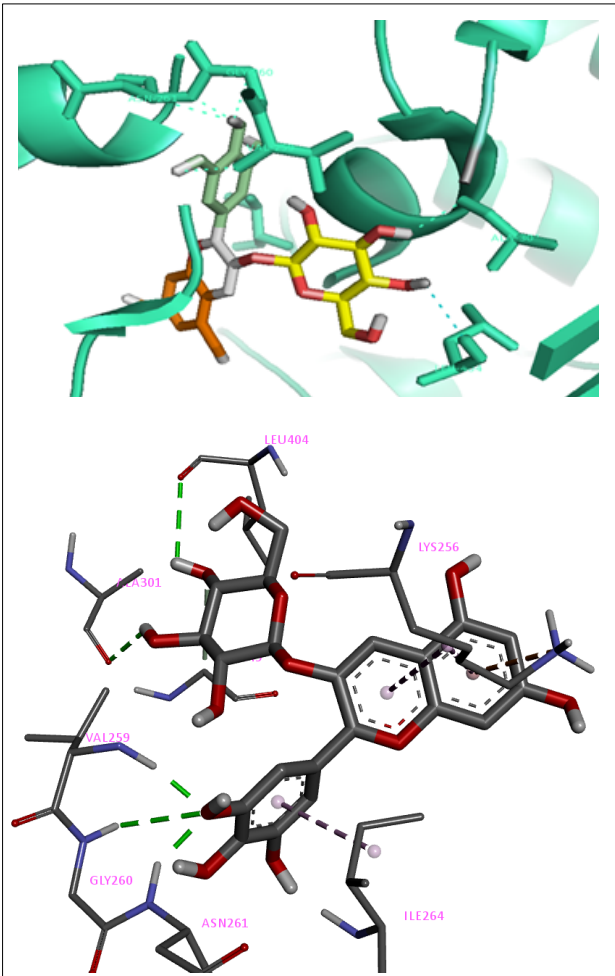


Figure 6: The different interactions: H-bonds π -alkyl, π -sigma and alkyl hydrophobic and electrostatic in cy-3-glu anthocyanin. Bonds are represented by dashed lines; classical H-bonds are in green; C-H bonds in grey, π -sigma dark violet, π -cation orange, π -alkyl violet, and alkyl faint violet.

According to Kostić et al.¹⁵, the absence of a hydroxyl group in the anthocyanins at C-3 position, as shown in Figure 1, is the main factor influencing the inhibitory activity of all anthocyanins.

Dp-3-rhm is characterised over other ligands by the presence of hydroxyl groups at C-5 and C-7 and a double bond between C-2 and C-3. These are essential requirements for its high inhibitory activity toward XO, as reported by Kostić et al.¹⁵

The strong inhibitory activity of the anthocyanin ligands towards XO suggests the use of anthocyanins as components of potential drugs as superior to the standard hyperuricaemia drug, topiroxostat. The interactions of ligands and topiroxostat toward the enzyme are given in Figure 7.

Acknowledgements

We thank the LC-MS Laboratory, Beijing University of Chemical Technology, China, for the identification analysis via LC-MS/MS. We also thank Dr Sed Ahmed Osman, El-Neelain University, Khartoum, Sudan.

Competing interests

We have no competing interests to declare.

Authors' contributions

A.E-N.: Conceptualisation, formulation or evolution of overarching research goals and aims; methodology development and design; chemical and computational experiments and analysis; data collection; sample preparation and analysis; data analysis; writing – the initial draft (including substantive translation); validation. S.A.: Conceptualisation, formulation or evolution of overarching research goals and aims; writing – revisions; project management; student supervision. I.A.: Project management; student supervision. G.A.: Phytochemistry.

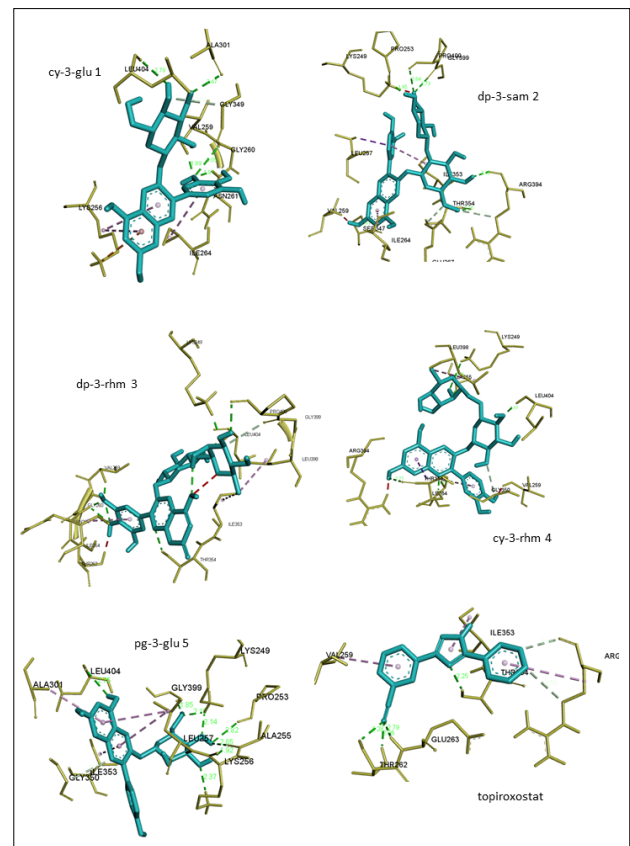


Figure 7: Binding interactions of the ligands cy-3-glu 1, dp-3-sam 2, dp-3-rhm 3, cy-3-rhm 4, pg-3-glu 5 and topiroxostat. Hydrogen bonds between the binding amino acid residues at the flavin adenine dinucleotides binding site and ligands. The ligand structures are shown in light blue, amino acid residues in pale yellow, and classical H-bonds are in green.

References

1. Mohamed BB, Sulaiman AA, Dahab AA. Roselle (*Hibiscus sabdariffa* L.) in Sudan, cultivation and their uses. *Bull Env Pharmacol Life Sci*. 2012;1:48–54.
2. Okereke CN, Iroka FC, Chukwuma MO. Phytochemical analysis and medicinal uses of *Hibiscus sabdariffa*. *Int J Herb Med*. 2015;2:16–19.
3. AL-Shoosh WGAA. Chemical composition of some roselle (*Hibiscus sabdariffa*) genotypes [thesis]. Khartoum: University of Khartoum; 1997.
4. Abou-Arab AA, Abu-Salem FM, Abou-Arab EA. Physico-chemical properties of natural pigments (anthocyanin) extracted from roselle calyces (*Hibiscus sabdariffa*). *J Am Sci*. 2011;7:445–456.
5. Riaz G, Chopra RA. Review on phytochemistry and therapeutic uses of *Hibiscus sabdariffa* L. *Biomed Pharmacother*. 2018;102:575–586. <https://doi.org/10.1016/j.biopha.2018.03.023>
6. Obouayeba AP, Djyh NB, Diabate S, Djaman AJ, N'Guessan JD, Kone M, et al. Phytochemical and antioxidant activity of roselle (*Hibiscus sabdariffa* L.) petal extracts. *Res J Pharm Biol Chem Sci*. 2014;5:1454.
7. Zia-Ul-Haq M, Riaz M, Saad B. Anthocyanins and human health: Biomolecular and therapeutic aspects. Cham: Springer International Publishing; 2016. <https://doi.org/10.1007/978-3-319-26456-1>
8. Hirsch GE, Martins LAM. Anthocyanins: Chemical features, food sources and health benefits. In: *Handbook of anthocyanins*. New York: Nova Science Publishers; 2015. p. 227–248.
9. Welch CWuQ, Simon J. Recent advances in anthocyanin analysis and characterization. *Curr Anal Chem*. 2008;4:75–101. <https://doi.org/10.2174/157341108784587795>
10. Harborne JB. *Phytochemical methods: A guide to modern techniques of plant analysis*. 3rd ed. London: Chapman and Hall; 1998.
11. Ingrid HM, Jaka, Santoso H. Natural red dyes extraction on roselle petals. *IOP Conf Ser Mater Sci Eng*. 2016;162:012029. <https://doi.org/10.1088/1757-899X/162/1/012029>
12. Kong JM, Chia LS, Goh NK, Chia TF, Brouillard R. Analysis and biological activities of anthocyanins. *Phytochemistry*. 2003;64:923–933. [https://doi.org/10.1016/S0031-9422\(03\)00438-2](https://doi.org/10.1016/S0031-9422(03)00438-2)
13. Hopkins AL, Lamm MG, Funk JL, Ritenbaugh C. *Hibiscus sabdariffa* L. in the treatment of hypertension and hyperlipidemia: A comprehensive review of animal and human studies. *Fitoterapia*. 2013;85:84–94. <https://doi.org/10.1016/j.fitote.2013.01.003>
14. Wallace TC. Anthocyanins in cardiovascular disease prevention. In: *Handbook of anthocyanins in health and disease*. London: Taylor and Francis; 2014. p. 165–198.
15. Kostić DA, Dimitrijević DS, Stojanović GS, Palić IR, Đorđević AS, Ickovski JD. Xanthine oxidase: Isolation, assays of activity, and inhibition. *J Chem*. 2015;2015:1–8. <https://doi.org/10.1155/2015/294858>
16. Umamaheswari M, Madeswaran A, Asokkumar K, Sivashanmugam T, Subhadradevi V, Jagannath P. Discovery of potential xanthine oxidase inhibitors using in silico docking studies. 2011;3:240–247. <https://doi.org/10.3329/bjp.v7i1.10007>
17. Gliozzi M, Malara N, Muscoli S, Mollace V. The treatment of hyperuricemia. *Int J Cardiol*. 2016;213:23–27. <https://doi.org/10.1016/j.ijcard.2015.08.087>
18. Wrolstad RE, Acree TE, Decker EA, Penner MH, Reid DS, Schwartz SJ. Pigments and colorants. In: *Handbook of food analytical chemistry*. Hoboken, NJ: John Wiley and Sons; 2004. p. 1–69. <https://doi.org/10.1021/ja059701s>
19. Sofowara A. Screening plants for bioactive agents. In: *Medicinal plants and traditional medicine in Africa*. Ibadan: Spectrum Books Ltd; 1993. p. 134–156.
20. Jork H, Funk W, Fischer W, Wimmer H. Physical and chemical detection methods: Fundamentals. In: *Thin-layer chromatography: Reagents and detection methods*. Weinheim: VCH; 1990.
21. Wolfe K, Wu X, Liu RH. Antioxidant activity of apple peels. *J Agric Food Chem*. 2003;51:609–614. <https://doi.org/10.1021/jf020782a>
22. Shanmukha I, Patel J, Settee RS. Spectroscopic determination of total phenolic and flavonoid contents of *Sesbani afrandiflora* (Linn) flower. *Am J Pharm Tech Res*. 2012;2:399–405.
23. Cahlíková L, Ali BH, Havlíková L, Ločárek M, Siatka T, Opletal L, et al. Anthocyanins of *Hibiscus sabdariffa* calyces from Sudan. *Nat Prod Commun*. 2015;10:77–79. <https://doi.org/10.1177/1934578X1501000120>
24. Bisht N, Singh BK. Role of computer aided drug design in drug development and drug discovery. *Int J Pharm Sci Res*. 2018;9:1405–1415.
25. Pagadala NS, Syed K, Tuszynski J. Software for molecular docking: a review. *Biophys Rev*. 2017;9:91–102. <https://doi.org/10.1007/s12551-016-0247-1>
26. Trott O, Olson AJ. AutoDock Vina: Improving the speed and accuracy of docking with a new scoring function, efficient optimization, and multithreading. *J Comput Chem*. 2010;31:455–461. <https://doi.org/10.1002/jcc.21334>
27. Berman HMJ, Westbrook J, Feng Z, Gilliland GTN, Bhat GTN, Weissig H, et al. The Protein Data Bank. *Nucleic Acids Res*. 2000;28:235–242.
28. Kim S, Chen J, Cheng T, Gindulyte A, He J, He S, et al. PubChem 2019 update: Improved access to chemical data. *Nucleic Acids Res*. 2019;47:1102–1109. <https://doi.org/10.1093/nar/gky1033>
29. Pettersen EF, Goddard TD, Huang CC, Couch GS, Greenblatt DM, Meng EC, et al. UCSF Chimera – a visualization system for exploratory research and analysis. *J Comput Chem*. 2004;25:1605–1612. <https://doi.org/10.1002/jcc.20084>
30. O'Boyle NM, Banck M, James CA, Morley C, Vandermeersch T, Hutchison GR. Open Babel: An open chemical toolbox. *J Chem Inf*. 2011;3:33. <https://doi.org/10.1186/1758-2946-3-33>
31. Sanner MF. Python: A programming language for software integration and development. *J Mol Graphics Mod*. 1999;17:57–61.
32. Diego S. Dassault Systèmes BIOVIA, Discovery Studio Visualizer, 2016.
33. The PyMOL Molecular Graphics System, Version 1.2r3pre, Schrödinger, LLC.
34. Salem MZM, Olivares-Pérez J, Salem AZM. Studies on biological activities and phytochemicals composition of *Hibiscus* species – A review. *Life Sci J*. 2014;5:1–8.
35. Alamin YK. Physicochemical study of *Hibiscus sabdariffa* L. (Karkade) genotypes [thesis]. Khartoum: University of Khartoum; 2012.
36. Obouayeba AP, Okoma KM, Diarrassouba M, Diabaté S, Kouakou TH. Phytochemical characterisation and antioxidant activity of *Hibiscus sabdariffa* (Malvaceae) calyx extracts. *JAAS*. 2015;3:39–46.